1   **Coincident beach surveys using UAS, vehicle mounted and airborne laser scanner: point cloud**

2   **inter-comparison and effects of surface type heterogeneity on elevation accuracies**

3   Paul Elsner[a], Uwe Dornbusch[b], Ian Thomas[c], Dan Amos[d], James Bovington[d], Diane Horn[a]

4   [a]Birkbeck, University of London, Department of Geography, Environment and Development Studies,

5   Malet Street, London WC1E 7HX, UK

6   [b] Environment Agency, Worthing, BN11 1LD, UK

7   [c] Pevensey Coastal Defence Ltd, Environment Agency Depot, Coast Road, Pevensey Bay, East Sussex

8   BN24 6ND, UK

9   [d] Strategic Regional Coastal Monitoring Programme, Adur and Worthing Councils, Worthing Town

10   Hall, Chapel Road, Worthing, West Sussex BN11 1HA, UK

11   **Abstract**

12   Reliable and consistent topographic data is key to a multitude of environmental manangement and research

13   applications. Unmanned Aerial Systems (UAS) are fast establishing themselves as a promising additional

14   remote sensing platform that provides high spatial resolution not only of topography but also surface types

15   and coastal features together with comparatively low costs and high deployment flexibility. However,

16   comprehensive information on the accuracy of UAS-based elevation models in comparison to other available

17   surveying methodology is regulary limited to be referenced to individual methods. This paper addresses this

18   shortcoming by comparing coincident beach surveys of three different point cloud generating methods: ATV

19   mounted mobile laser scan (MLS), airborne LiDAR (ALS), and UAS. This was complemented by two RTK-GPS

20   surveys on a pole with wheel attachment and mounted on an ATV.

21   We present results in relation to elevation accuracies on a concrete control surface, the entire beach and for

22   six different beach surface types together with how differences between point clouds propagate during the

23 construction of gridded elevation models. Overall, UAS point cloud elevations were consistently higher than

24 those of ALS (+0.063 m) and MLS (+0.087 m). However, these results for the entire beach mask larger and

25 smaller differences related to the individual surface characteristics. For all surface types, UAS records higher

26 (from 0.006 m for wet sand to 0.118 m for cobbles, average of 0.063 m) elevations than ALS. The MLS on the

27 other hand, records predominantly lower elevation than ALS (-0.005 m for beach gravel to -0.089 m for soft

28 mud, average of -0.025 m) except for cobbles, where elevations are 0.056 m higher.

29 The comparison shows that all point cloud methods produce elevations that are suitable for monitoring

30 changes in beach topography in the context of operational coastal management applications. However, due

31 to the systematic differences between respective monitoring approaches, care needs to be taken when

32 analysing beach topographies for the same area based on different methods.

33 The eventual choice of monitoring method is therefore guided by a range of practical factors, including

34 capital cost of the system and operating costs per survey area, conditions under which the system can

35 operate, data processing time, and legal restrictions in the use of the system such as air safety regulations or

36 limitation of ground access to areas with environmental protection.

37 **1. Introduction**

38 The high variability of natural environments such as beaches at a wide range of temporal and spatial scales in

39 relation to, for example, topography and surface characteristics (Dornbusch et al., 2008; Watt et al., 2008)

40 presents a substantial challenge to their monitoring. Historically, ground survey methods ranging from

41 simple one person approaches (Delgado and Lloyd, 2004) to optical methods (Anderson et al., 1998) to GNSS

42 point collection (Goncalves et al., 2012) have been used to monitor fixed profiles due to the time

43 requirements to record individual points. The more rapid point acquisition using GNSS together with surface

44 interpolation software has meant that different sampling strategies including mounting the receiver on

45 vehicles such as All Terrain Vehicles (ATV) can be used to represent full 3D surfaces rather than individual

46 profiles (Dornbusch, 2010). Recent developments also include the analysis of laser return intensity in the

47 analysis and offer a range novel applications of Lidar remote sensing beyond 3-D (Eitel et al., 2016).

48 Finally, advances in the field of Unmanned Aerial Systems (UAS) are now emerging as a promising additional

49 remote sensing platform that provides high spatial resolution not only of topography but also surface

50 characteristics and coastal features (Papakonstantinou et al., 2016). Since it is also comparatively low-cost

51 and very flexible in terms of deployment (Mancini et al., 2013; Micheletti et al., 2015a; Nex and Remondino,

52 2014) it has as a consequence started to become the method of choice for some coastlines (Gonçalves and

53 Henriques, 2015; Turner et al., 2016).

54 A central advantage of the UAS approach is that two data sets can be acquired at the same time: (i) multi-

55 spectral data sets which capture information about the spatial distribution of surface characteristics such as

56 the spatial distribution and patterns of sand and gravel at mixed beaches, and (ii) elevation models using

57 novel photogrammetric approaches such as Structure-from-Motion (SFM) (Westoby et al., 2012) that relax

58 many of the prerequisites of classical digital photogrammetry. The potential for the use of unmanned aerial

59 systems for coastal monitoring has been recognised for a number of years and the use of UAS is becoming

60 increasingly common (Brunier et al., 2016; Harwin and Lucieer, 2012; Klemas, 2015; Lim et al., 2015; Mancini

61 et al., 2013; Pereira et al., 2009). However, comprehensive information on the accuracy of UAS-based

62 elevation models in comparison to other available surveying methodology is limited. Reports of how UAS

63 projects perform in operational circumstances against other surveying methods often only compare UAS-

64 based elevation individually against those derived from Total Station (Harwin and Lucieer, 2012), RTK-GNSS

65 (Gonçalves and Henriques, 2015; Turner et al., 2016), or laser scanning (Flener et al., 2013; Mancini et al.,

66 2013). This paper aims to address this shortcoming by reporting for the first time comparisons of surveys of

67 five different methods carried out within a one hour time window: three point cloud generating methods

68 (ATV mounted mobile laser scan, airborne LIDAR and UAS), complemented by two line transects collected

69 with a RTK-GNSS on a pole with wheel attachment and a RTK-GNSS mounted on an ATV. We present results

70 in relation to elevation accuracy overall and for different surface characteristics. The implications of these

71   results for are explored for both the construction of elevation models and planning and implementation for

72   future scientific studies, particularly in the coastal management context.

73   **2. Experimental set-up and methodology**

74   Study site

75   The study was carried out covering an area of 65,500 m^2 along an approximately 450 m long stretch of the 9

76   km long shingle barrier at Pevensey Bay, East Sussex, UK (Fig. 1). The south-east facing beach is in a

77   macrotidal environment with a mean spring tide range of over 6 m and an average annual maximum

78   offshore wave height (0.05 % exceedance) of ~4 m.
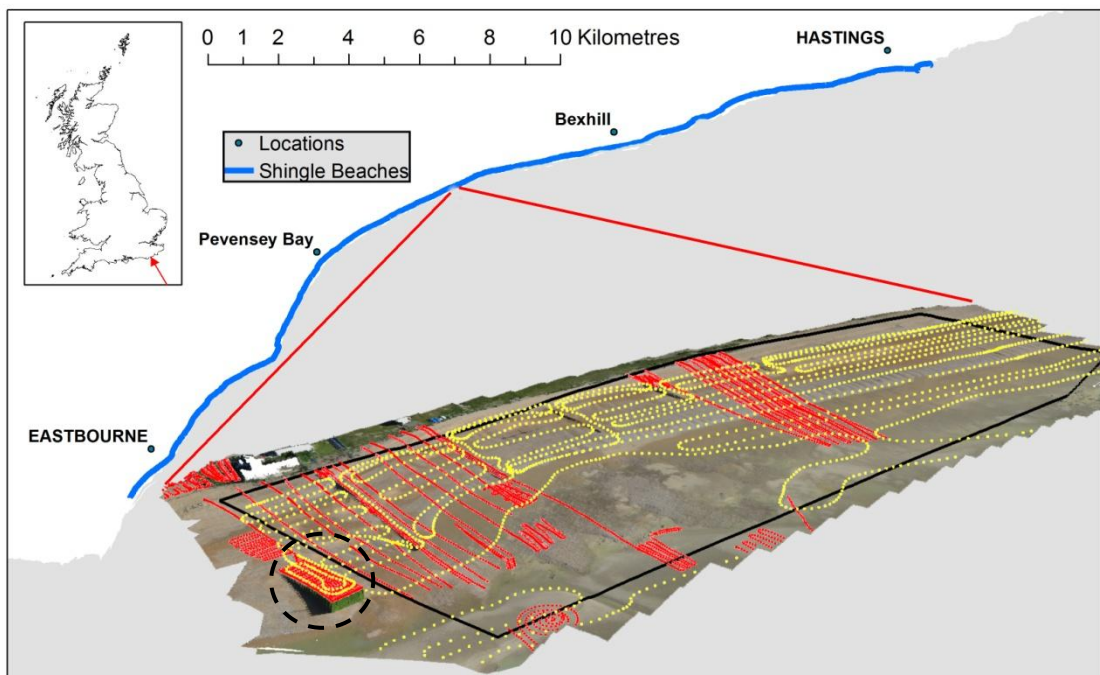
79

80   **Fig. 1.** Overview map and orthophoto of the study area, generated from UAS images. Yellow dots represent data

81   collected with ATV-based RTK-GNSS, red dots represent data collected with pole-based RTK-GNSS. The black box

82   outlines actual study area. Dashed circle depicts sluice outfall with concrete surface that was used as test surface.

4

83   The beach profile at Pevensey can best be described as a composite mixed beach where the reflective upper

84   beach (beach toe at approximately -1.5 m OD) is composed of mixed sand and gravel, fronted by a very

85   shallow gradient, dissipative and mostly sand covered low-tide terrace (Watt et al., 2008) that in this location

86   is underlain by intertidal back barrier sediments and sandstone over which the barrier has rolled back (Fig.

87   2). The surface sediment on the upper beach face can change over the course of a tide from a several

88   decimetre thick pure gravel layer to a very hard surface layer of mixed sand and gravel with both types

89   commonly found at the same time on different parts (cross-shore and longshore) of the beach (Dornbusch et

90   al., 2008; Watt et al., 2008).

91   Pevensey Bay beach acts as a natural sea defence which provides protection from permanent flooding to an

92   area of 50 km^2, most of which is significantly below high tide level. The beach is managed through recharge,

93   reprofiling and recyling of sediment within the frontage. The field site was chosen because it represents are

94   an example of a rapidly changing dynamic coastal environment that requires monitoring on a regular basis. It

95   also exhibits a range of different surface types which makes it possible to investigate the influence surface

96   variation on surveying accuracy. The presence of a nearby concrete outfall offered additionally the

97   opportunity to calibrate measurements to such control surface.

98

99

100   **Fig. 2.** View down beach with the mixed beach in the foreground and the low tide terrace in the background. The two

101   near parallel wheel traces are from the ATV_GNSS and were the first, the strongly curved one is from the MLS, which

102   came second, and the thin line with foot prints going up the beach to its right in the centre of the photos are from the

103   W-GNSS coming last.

104   Five concurrent surveys were carried out on the morning of May 20, 2015 during low water spring tide.

105   These were:

106   a) Cross-shore beach transects collected with a wheel-based RTK-GNSS (W-GNSS):

107   The instrument set-up and survey strategy follows that described in Dornbusch (2010) using a 0.28m

108   diameter wheel attached to a 1.8 m high survey pole with a Leica 1200 sampling at 1Hz (Fig. 3a). Walking

109   speed and thus point density along the path was adjusted to the change in topography. This method relies

110   on the contact with the beach surface and the constant distance between surface and GNSS receiver, so the

111   main source of elevation errors comes from the GNSS sensor, but also from minor sinking in of the wheel on

112   different sediment types (Fig. 2), pole non verticality and the surface wheel contact point moving away from

113   vertically under the antenna on steeper slopes.

114   b) Longshore beach transects collected by ATV-based RTK-GNSS (ATV-GNSS):

115   Longshore transects were collected using a Trimble R8 receiver mounted on an ATV (Fig. 3b). Individual

116   points were collected using Trimble's "Continuous Topo" mode, sampling at 1 Hz. The typical driving speed

117   was 2.7 – 5.4 ms^{-1}. The receiver was mounted 1.4 m above ground level as close as possible to the front left

118   wheel of the ATV, so that as long as the wheel stayed in contact with the beach, the receiver height was

119   relevant. Data resulting from these surveys is processed through a bespoke software package developed by

120   McCarthy Taylor Systems Ltd. which corrects for non-verticality of the mounting pole. Like the W-GNSS

121   method it relies on the contact with the beach surface and constant distance between surface and GNSS

122   receiver. ATV wheels do sink into the beach surface but this was somewhat limited due to very low pressure

123   in the tyres. Nevertheless, on pure gravel the sinking distance could reach several centimetres, especially in

124   curves (Fig. 2) . In addition, the wheel suspension system introduces variations of the constant distance.

125   c) ATV-based mobile laser scanning (MLS):

126   The MLS set-up consisted of a single head MDL Dynascan Laser Scanning System (M250) including a laser

127   scanning module (with a pulse rate of 36 kHz at 1200 rpm), an Inertial Measurement Unit (IMU) and two

128   GNSS receivers for position and heading data mounted on an ATV (Fig. 3c). The instrument is mounted 2 m

129   above the surface. The footprint of the laser on the ground changes rapidly with distance, but is generally in

130   the order of 0.1 m at a distance of 50 m (Renishaw, 2016). The driving speed varied between 4 - 10 ms^{-1}. The

131   MLS system is operated by the Worthing Borough Council Coastal Survey Team and has been used for

132   routine beach surveys since 2013. The sinking in of the vehicle is similar to that for the ATV-GNSS (Fig. 2) ,

133   but is of no consequence as beach elevation is measured relative to the GNSS position of the instrument.

134   d) Airborne laser scanning (ALS) on board a survey aircraft:

135   ALS data was collected by the Geomatics team of the UK Environment Agency using an Orion Airborne Laser

136   Terrain Mapper flown on a Cessna 406 (G-LEAF, Fig. 3d). Flights were carried out at 900 m above ground at a

137   speed of 260 kmh^{-1} with a scanning frequency of 40kHz and a scan angle of 50°. Flight paths were parallel to

138   the coast with an overlap of 30 percent. The survey covered the entire length of Pevensey Bay which

139   included two ground control areas outside the study area.

140   The potential source of error for ALS measurements lies in the GNSS positioning of the plane, pitch, roll and

141   yaw of the plane compensated through an IMU and adjustment of flightpaths against each other, laser

142   measurement itself and the signal footprint of approximately 0.2 m diameter.

143   e) A multi-rotor UAS platform, represented by a Tarot 680Pro series Arducopter GNSS Hexacopter (Fig. 3e)

144   carrying a Canon PowerShot A2300 16.0 megapixel camera. The copter was equipped with a Pixhawk flight

145   controller and a GNSS module with compass. This allowed it to carry out pre-programmed autonomous

146   survey missions using the software Mission Planner (Oborne, n.d.). The survey itself was carried out in

147   autopilot mode during which the UAS flew at a height of approximately 70 m above ground, which resulted

148   in a final data set of 145 images with a ground sampling distance (GSD) of 1.7 cm per pixel and a minimum

149   overlap of 60 percent in both the side- and forward direction.. The images were then processed using the

150   SFM-based package Photoscan (Agisoft Photoscan, 2015).   It performs an automatic camera calibration by

151   estimating both internal and external camera orientation parameters, including nonlinear radial distortions

152   based on the images EXIF meta data. Surface construction was carried out in a three step process, starting

153   with image alignment by detecting and matching common feature points across images. The establishment

154   of this basic geometric structure resulted in computed camera positions and a sparse point cloud. This was

155   followed by the generation of a dense point cloud model, where the estimated camera

156   positions were used to calculate depth information for each image which was then combined into a single

157   dense point cloud for the entire surface. A number of quality settings were possible at this stage which

158   essentially offered trade offs between accuracy and computing speed. For this project the *Ultra High* option

159   was selected that ensured that the full photo resolution was utilised by the programme. The final step

160   consisted of building a three dimensional polygonal model mesh, based on the previously generated dense

161   point cloud and overlaying this with orthophoto texture which allowed the best visual representation of the

162   generated 3D model.

163   For a more detailed description of Agisoft and its underlying principles, the reader is referred to (Gonçalves

164   and Henriques, 2015).   A bundle adjustment transformation was eventually carried out to reference the

165   model to a British National Grid coordinate system using 49 ground control points, resulting in a vertical

166   RMSE of the residuals of 4.6 cm. The control points had been surveyed with a Leica Viva GS08 RTK- GNSS

167   receiver linked into the GNSS SmartNet Network RTK service. The points were placed on groins evenly

168   spread across the study area, as these represent semi-permanent features that could be reused for

169   subsequent surveys. This would mimic an approach that is likely to be taken in an operational surveying

170   setting.

171

172
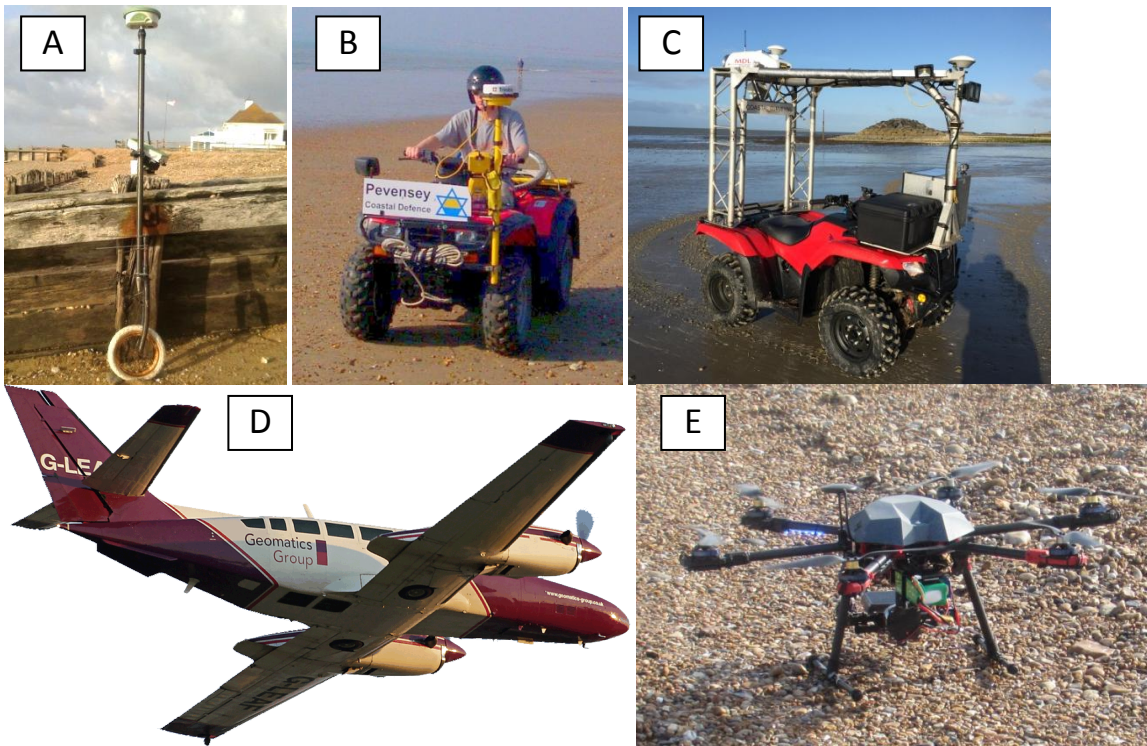
173   **Fig. 3.** Survey methods deployed concurrently at the study area: (A) wheel-based RTK-GNSS (W-GNSS), (B) ATV-based

174   RTK-GNSS, (C) mobile laser scanning using sensors mounted on an ATV (MLS), (D) airborne laser scanning (ALS), and (E)

175   multi-rotor UAS.

176

177   The W-GNSS transects resulted in 5613 points, and the transect surveyed with ATV-GNSS collected 2427

178   points, both shown in Fig. 1. The MLS point cloud of the study area consisted of 5.3 million points, equivalent

179   of an average of 112 points/m^2. However, the density of the MLS point cloud varied substantially, with some

180   sections of the foreshore being captured very sparsely (Fig. 4a), due to surface wetness where signal return

181   away from the scanner deteriorated substantially. ALS collected 270,000 points within the case study area

182   with a homogeneous distribution. This equalled a point density of approximately 4 points per m^2. The UAS-

183   based surface model was generated using an image overlap pattern where all parts of the study area were

184   imaged from at least three perspectives and most of them by many more (Fig. 4b). The resulting point cloud

185   had a homogeneous distribution and was represented by 3.8 million points within the study area. This

186   translated into an average density of 58 points per m^2.

187   a   b
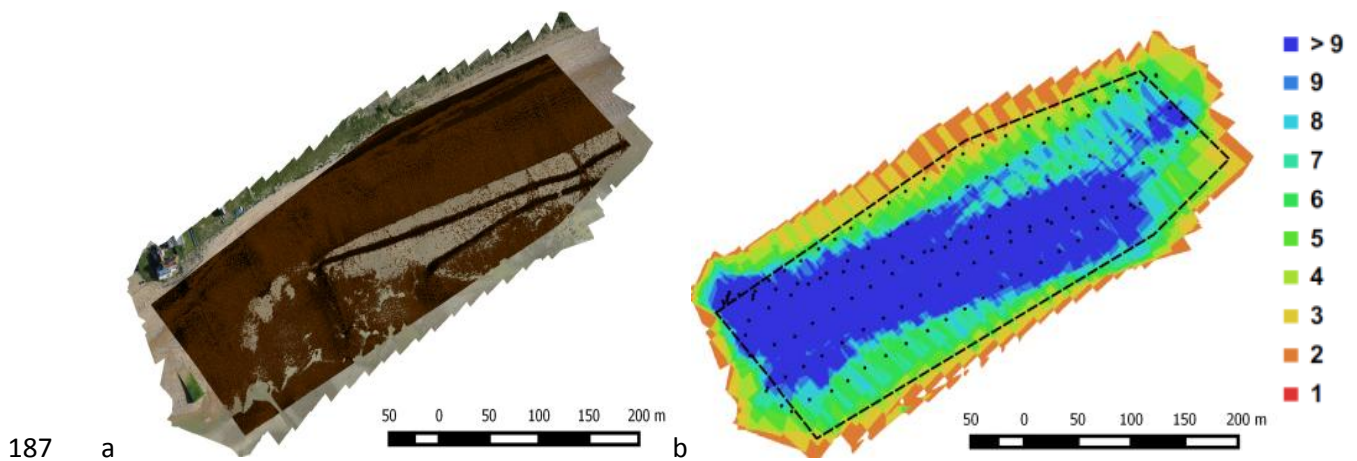
188   **Fig. 4.** Point cloud footprints generated by MLS (a) and camera locations and image overlap of the UAS survey (b). The

189   dashed line outlines the actual study area.

190   The central objective of this paper was to compare the elevation accuracy of the presently used methods of

191   airborne laser scanning and terrestrial laser scanning with that of the new UAS-based surface modelling so

192   that conclusions can be drawn for practical aspects of operational beach monitoring. This included the

193   calculation of the root-mean-square error (RMSE):

$$RMSE = \sqrt{\frac{\sum_{i=1}^{n}\left(h_g - h_p\right)^2}{n}}$$

194   where h_g represents the height value measured by respective GNSS devices and h_p represents height value
195   from respective point clouds.

196   The data analysis was carried out in a set of subsequent steps, consisting of (i) comparison of point cloud

197   performance against W-GNSS and ATV-GNSS data collected on a concrete control surface; (ii) comparison of

198   point cloud performance against both W-GNSS data and the ATV-GNSS on the actual beach study area; (iii)

199   point cloud inter-comparison, including the consideration of different surface types; and (iv) an evaluation of

200   differences between elevation models generated from the respective point clouds.

201   **3. Results**

202   **3.1 Comparison of W-GNSS and ATV-GNSS data with point clouds**

203   The relative elevation accuracy between RTK-GPS data and respective point clouds was first estimated on the

204   homogeneous 30 m x 10 m concrete surface of a sluice outfall immediately to the west of the actual beach

205   study area (see Fig. 1). Common point pairs for each data set combination were identified which where

206   within a maximum distance of 0.2 m from each other. This was based on the assumption that, on the

207   concrete surface, elevation differences between point pairs would be a function of survey methodology

208   alone and not of actual changes of the surface over such a short distance.

209   The analysis started with a comparison using W-GNSS data which is taken as the most accurate due to the

210   least number of error sources. Table 1 lists the satellite constellation conditions during the three phases of

211   the W-GNSS survey, i.e. (i) a survey of the concrete test surface surveying the study area; (ii) a subsequent

212   survey of the study area itself; and (iii) a repeat survey of the concrete test surface at the end. It can be seen

213   that all surveys experienced good conditions, with the study area itself experienced the most favourable and

214   stable constellation with a geometric dilution of precision (GDOP) between 2.4 and 3.4.

215   Real-time kinematic (RTK) corrections of the GNSS measurements were carried out by utilizing a set of

216   permanent and continuously operating OSNET reference stations. Six stations with a spacing of less than 70

217   kilometres were used to develop a virtual reference station. The WGS84 reference system was used for all

218   surveys.

11

219   **Table 1.** Satellite constellation conditions for the different phases of the W-GNSS survey, stating the range of geometric

220   dilution of precision (GDOP), vertical dilution of precision (VDOP), horizontal dilution of precision (HDOP), and position

221   dilution of precision (PDOP).

W-GNSS survey	GDOP	VDOP	HDOP	PDOP	Satellites used
Survey concrete test surface (start)	2.3 - 4.2	2.6 - 3.2	1.3 - 1.9	1.8 - 3.6	7 (GPS)
Survey study area	2.4 - 3.4	1.7 - 2.4	1.2 -1.6	2.0 -2.9	10 (GPS)
Survey concrete test surface (end)	2.3 - 4.1	1.6 - 3.0	1.1 - 1.6	1.9 - 3.4	9 (GPS)

222

223   The results of the accuracy analysis are displayed in Table 2. The best agreement was observed for the ALS

224   point cloud elevation, where W-GNSS data was on average 0.016 m lower, with a RMSE error of 0.026 m and

225   a standard deviation (STD) of 0.021 m. This comparison consists of two sets of W-GNSS data, one collected at

226   the start of the survey and one collected 2 hours later at the end of the survey, denoted 'start' and 'end' in

227   Table 1. For the other comparisons this split is not shown. There is a 0.007 m systematic difference between

228   the two data sets and a 0.01m difference in the RMSE. The UAS-based point cloud showed a mildly higher

229   difference of 0.023 m (RMSE 0.054 m and STD 0.049 m). The point cloud generated by ground-based mobile

230   laser scanning exhibited the highest average difference with W-GNSS data being 0.072 m lower (RMSE 0.094

231   m, STD 0.061 m).

232   The analysis between ATV-GNSS and point clouds resulted in a similar pattern, with ALS data being the most

233   consistent (average difference -0.026 m, RMSE 0.038 m), followed by the UAS point cloud (average

234   difference -0.034 m, RMSE 0.074 m) and MLS points (average difference -0.094 m, RMSE 0.107 m).

235   Finally, the accuracy of ATV-GNSS points was tested against the W-GNSS points, using the same approach as

236   described above. This resulted in an excellent agreement with an average vertical difference of 0.005 m

237   (RMSE 0.025 m), indicating that the two contact methods produced nearly identical results on the control

238   surface (Table 2).

239 **Table 2**

240 Difference of point cloud elevations as estimated against the contact methods for the concrete control surface and the

241 beach study area, based on common points within a 0.2m circle (concrete test surface) and 0.1 m (beach study area).

242 Negative values for the average difference mean that the elevation of the GNSS method is lower than the respective

243 point cloud. For example, in the first row, the W-GNSS elevations were on average 0.023 m lower than those of the UAS

244 survey.

		Average difference (m)	RMSE (m)	STD (m)	Min (m)	Max (m)	Sample size
W-GNSS - UAS	test surface	-0.023	0.054	0.049	-0.182	0.144	439
W-GNSS - MLS	test surface	-0.072	0.094	0.061	-0.038	0.569	141
W-GNSS - ALS	test surface	-0.016	0.026	0.021	-0.051	0.07	179
W-GNSS – ALS (start)	test surface	-0.012	0.02	0.016	-0.031	0.053	95
W-GNSS – ALS (end)	test surface	-0.019	0.03	0.02	-0.051	0.069	84
ATV-GNSS - UAS	test surface	-0.034	0.074	0.066	-0.197	0.274	78
ATV-GNSS - MLS	test surface	-0.094	0.107	0.053	0.027	0.244	19
ATV-GNSS - ALS	test surface	-0.026	0.038	0.028	-0.014	0.082	22
W-GNSS - ATV-GNSS	test surface	0.005	0.025	0.025	-0.064	0.043	29
W-GNSS - UAS	Study area	-0.053	0.113	0.1	-0.272	0.745	3567
W-GNSS - MLS	Study area	-0.001	0.145	0.145	-1.47	0.155	1772
W-GNSS - ALS	Study area	0.0001	0.036	0.036	-0.145	0.195	442

ATV-GNSS - UAS	Study area	-0.069	0.108	0.083	-0.225	0.683	1542
ATV-GNSS - MLS	Study area	-0.011	0.113	0.113	-1.809	1.153	881
ATV-GNSS - ALS	Study area	-0.005	0.036	0.036	-0.119	0.148	224

245

246 The second comparison of point cloud accuracy in reference to RTK-GNSS measurements was undertaken for

247 the case study beach area itself including both W-GNSS and the ATV-GNSS data. For this analysis, only point

248 groups within 0.1 m distance were employed, that is, a GNSS point was only used when all three point clouds

249 had an elevation measurement within a radius of 0.1m to the GNSS point. The reduction of the search

250 distance was motivated by the fact that on the beach itself morphological changes occur over much shorter

251 distances. For W-GNSS data, the ALS point cloud data again was the most accurate, both in terms of

252 elevation difference (-0.0001 m) and RMSE (0.036 m). For the UAS point cloud data both the average error (-

253 0.053 m) and RMSE (0.113 m) doubled in comparison to the concrete surface. MLS point cloud data had a

254 smaller average error (-0.001 m) but a much higher RMSE of 0.145 m.

255 The results for the analysis using the ATV-GNSS as benchmark partly repeat the results for the M-GNSS in

256 that the ALS point cloud had the smallest average error of -0.005 m (RMSE 0.036 m), the average error for

257 the UAS point cloud doubled to -0.069 m (RMSE 0.108 m), whereas the average error for the MLS point cloud

258 was lower with -0.011 m but the RMSE (0.113 m) was twice as high on the beach as on the concrete test

259 surface.

260 **3.2 Point Cloud inter-comparison**

261 The third step in the analysis focussed on the vertical differences between respective point cloud data sets

262 themselves. All point cloud analysis was carried out following an approach by Mancini et al. (2013) by

263 developing a MATLAB$^©$ routine which identified common point groups where points from all data sets under

264 investigation were identified that lay within a search circle radius of 0.1 m. This was based on the

265 assumption that actual morphological vertical changes within this short distance can be considered to be

266 minimal even on the beach. Any observed differences between data points could therefore be treated as a

267   function of data acquisition methodology alone. The search routine identified 1960 matches. Groins and

268   other man-made structures that could have had confounding influences were masked out.

269   The comparison of the two laser scanning point clouds shows a good agreement, with the MLS points being

270   on average 0.025 m (RMSE 0.069 m) lower compared to the ALS data (see Fig. 5). The spatial distribution of

271   the residuals shows a relative homogeneous distribution with a number of outliers being located along the
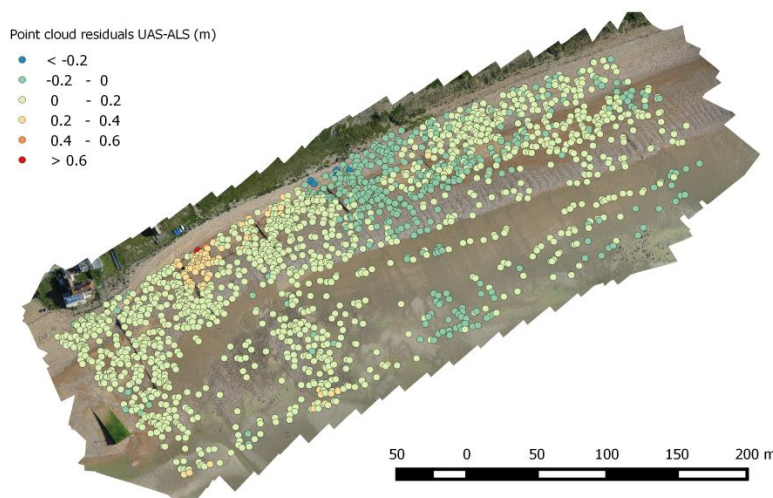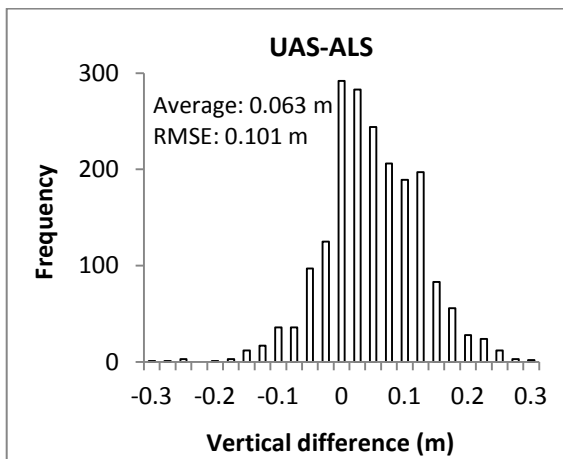
272   eastern part of the foreshore.

273
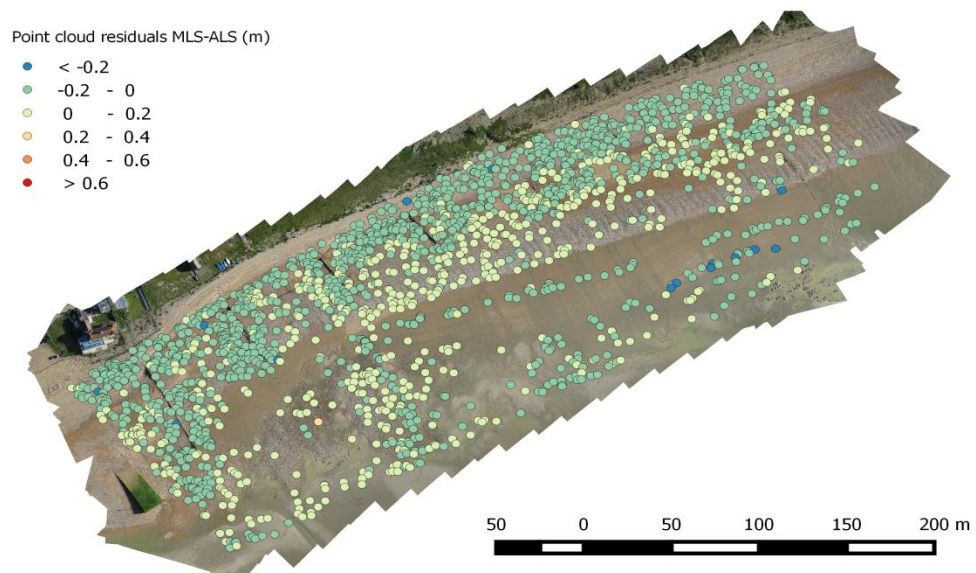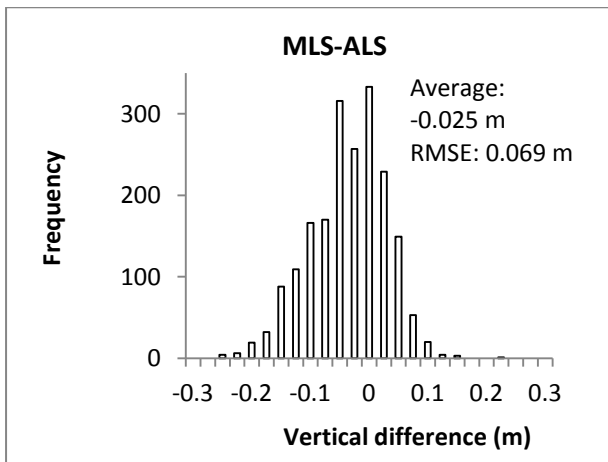
274
275   **Fig. 5.** Point cloud differences of MLS and ALS data (top), spatial distribution of residuals (bottom).

15

276

277　The differences between UAS data and ALS data are shown in Fig. 6. UAS data exhibited on average higher

278　elevations (+0.063 m) with a RMSE of 0.101 m. The spatial error pattern displays a cluster in the centre of the

279　case study area where UAS elevations are lower than ALS points, whereas in other areas this was the

280　opposite. In the south-western part of the study area on the upper shore there is a further small cluster of

281　approximately 20 m by 20 m where UAS points are substantially higher. The reason for this was not fully

282　clear but it is suggested that it be caused by a strong gust that disturbed the UAS platform in the respective

283　flight line.

284

285

Fig. 6. Point cloud differences of UAS and ALS data (top), spatial distribution of residuals (bottom).

Fig. 7 illustrates the differences between UAS and MLS point clouds. It can be seen that the UAS-based point cloud has a positive offset of +0.087 m compared to the MLS data with a RMSE of 0.132 m. The spatial distribution of the errors shows a feature in the centre of the beach area with a cluster where UAS data was consistently lower than the MLS points, whereas in the other areas this was reversed.
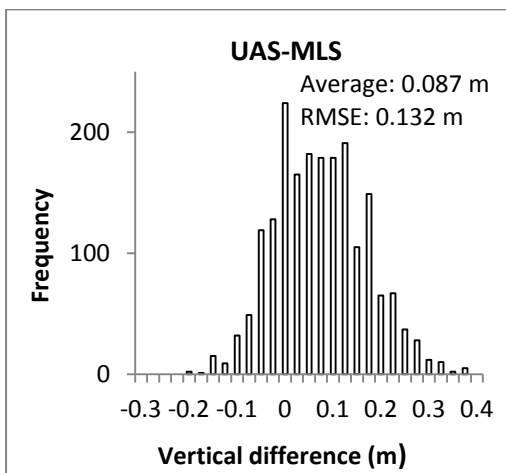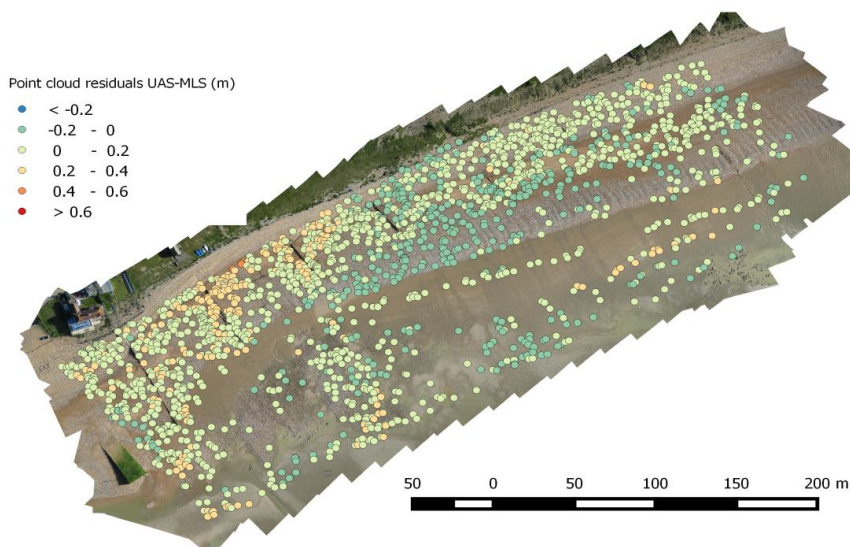
**Fig. 7.** Point cloud differences of UAS and MLS data (top), spatial distribution of residuals (bottom).

295

296 As the study area exhibits a complex mix of surface types, the fourth comparison was carried out to evaluate

297 to what extent surface variations had an effect on the measurement accuracy of the respective methods.

298 This relates back to observations in Dornbusch (2010) where a difference between contact based GNSS and

299 ALS data on concrete and pebble surfaces was observed. At the time of data acquisition, six different surface

300 types and their locations were identified. These were: *beach gravel,* defined as sections of the upper beach

301 that were homogenously covered with gravel (Fig. 2) ; *beach sand*, i.e. sections of the upper beach that had a

302 homogeneous sandy surface; *cobble* is a section on the lower shore where a coarse lag deposit of larger

303 clasts was exposed; *foreshore dry sand* marks areas of the lower foreshore that were slightly raised and

304 where the sand surface had dried out, while *wet sand* describes areas of the lower foreshore where a thin

305 film of water was still present on the surface during the surveys; *and soft mud* that relates to foreshore areas

306 consisting of soft and muddy substrate. Fig. 8 shows the sections for which it was possible to visually outline

307 the respective surface types with confidence from an orthophoto that was generated from the UAS images

308 and field observations on the day.
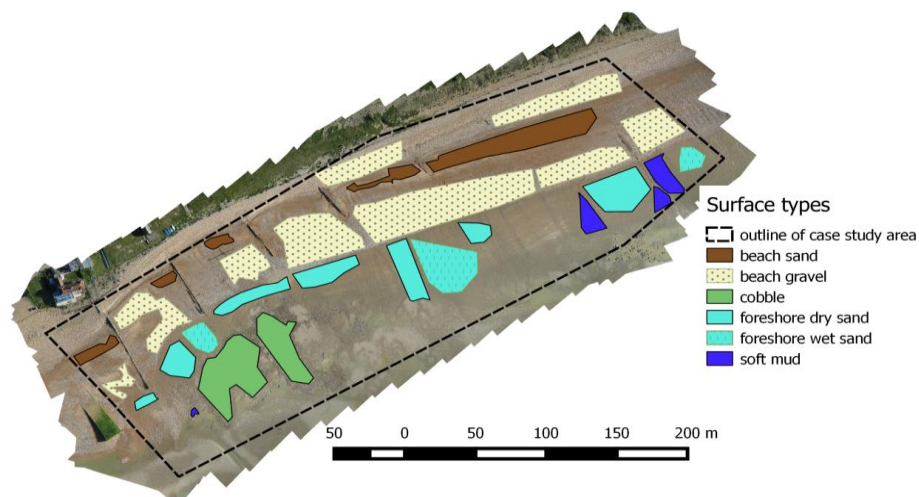
309

310 **Fig. 8.** Spatial distribution of surface types used for further analysis.

311

312   The results of this analysis are shown in Fig. 9 with the sample size for the respective surface type being

313   listed in Table 2. For all surface types, UAS records higher (from 0.006 m for wet sand to 0.118 m for cobbles,

314   average of 0.063 m) elevations than ALS. The MLS on the other hand, records predominantly lower elevation

315   than ALS (-0.005 m for beach gravel to -0.089 m for soft mud, average of -0.025 m) except for cobbles, where

316   elevations are 0.056 m higher. The differences for gravel, which forms the dominant surface type, are much

317   smaller for both UAS (0.038 m) and MLS (-0.005 m). Adjusting for the average difference and plotting the

318   ALS-UAS and ALS-MLS difference, both UAS and MLS show similar patterns of differences to the ALS survey

319   in relation to surface type. The cobble surface is the only one that shows much higher differences than the

320   average for both UAS and MLS; the three sand surfaces are all below average as is the soft mud area. The

321   only slight exception is the gravel surface that is slightly above average for the MLS survey but slightly below

322   average for the UAS survey.
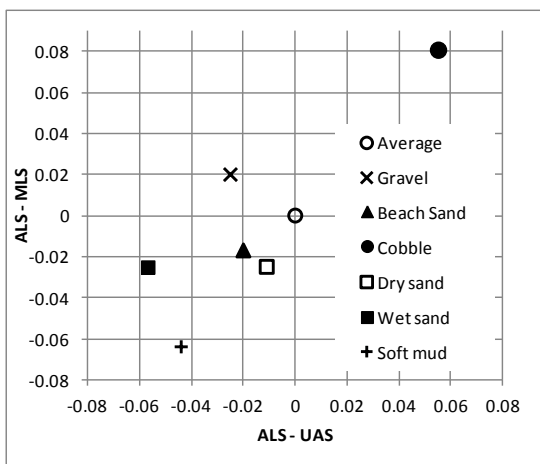
323

324   **Fig. 9.** ALS – UAS and ALS-MLS differences for different surface types from Table 2, adjusted for the beach average

325   difference for both comparisons.

326

327

328

329   **3.3 Elevation model differences**

330   In an operational coastal management context, survey point data are routinely converted to raster elevation

331   models at pre-specified resolutions to identify areas of beach sediment loss or gain at different spatial scales

332   and over different time periods. It is these data sets that are commonly analysed, visualised, and archived in

333   digital formats that can be incorporated and shared across many GIS platforms. It is therefore important to

334   understand how the observed differences in the primary point cloud data sets translate into interpolated

335   raster elevation models. To do this, we generated raster DEM models from each of the point clouds in three

336   spatial resolutions (0.2 m, 0.5 m, and 1 m), using the software package CloudCompare (Girardeau-Montaut,

337   2015). The height of each cell was determined by using the average height of all points falling in a grid cell.

338   'Empty' cells would be estimated by linear interpolation with the nearest non-empty neighbouring cells. This

339   was particularly necessary for the MLS exhibiting substantial gaps in the foreshore region (Fig. 4). The

340   differences between respective DEMs were analysed on a cell-by-cell basis and then aggregated.

341   Fig.10 shows that the differences from the point cloud analysis is only replicated in the UAS-ALS relationship

342   in that the average elevation difference is positive but slightly larger (0.07 m to 0.08 m for the different

343   DEMs compared to 0.06 m for the point cloud). For the DEM difference between MLS and ALS, the negative

344   difference of -0.02 m from the point cloud comparison changes to a positive difference of between 0.01 m to

345   0.05 m. There is also no obvious correlation between the magnitude of the difference and the cell size. In the

346   case of UAS against MLS data, the average differences of elevation models were smaller than the original

347   point cloud differences but showed no trend in terms of resolution.

348

349
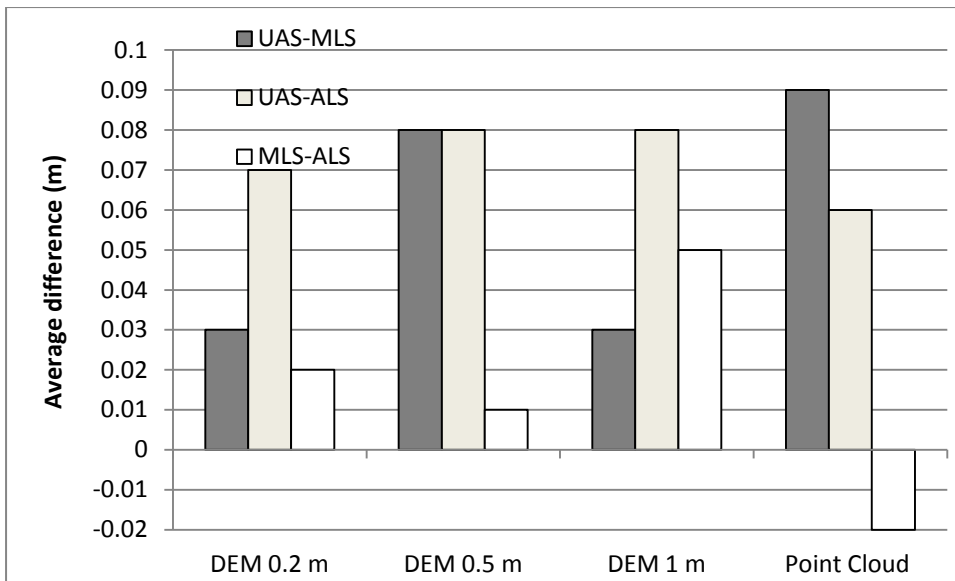
Fig. 10. Average differences of elevation models generated from respective point clouds. The error of the input point

351 cloud is given for reference.

352

4. Discussion

The results presented above show differences in elevation and calculated elevation models for the test

355 beach which we will discuss in relation to the terrain, surface characteristics and survey methods.

All instruments used in this study rely on GNSS positions and elevations obtained during movement, that is

357 no averaging during point occupation is possible. Dornbusch (2010) shows how elevations vary using the

358 same W-GNSS approach used in the present study between surveys over different time scales. While the ALS

359 and MLS elevations include measurements of the same surface at different times and thus provide some

360 averaging of the GNSS signal, the W- and ATV-GNSS survey cover each surface only with one pass and are

361 therefore more likely to include a GNSS bias. The only exception to this is the W-GNSS survey of the concrete

362 outfall surface and the difference with ALS in Table 1 confirms a centimetre scale difference between the

363 'start' and 'end' surveys. The UAS method employed in this study relies on GCP points collected in static

364 mode where GNSS averaging has taken place over 3 seconds. This means that any differences between

365 surveys within approximately ± 0.01 to 0.02 m are very likely to be associated with the uncertainty in the

21

366   GNSS system and that any difference between two methods associated with the whole method system have

367   to be larger than this.

368   The comparison between the contact methods on the concrete test survey show a very high degree of

369   agreement for common points with the W-GNSS only 0.005 m higher than the ATV-GNSS (Table 1). This is

370   based on 29 points that are within 0.2m of each other. A very similar result with W-GNSS being 0.01 m

371   higher than the ATV-GNSS is achieved by calculating the average elevation of the same surface using all 406

372   (W-GNSS) and 91 (ATV-GNSS) measurements taken. Given the general GNSS uncertainty, the two data GNSS

373   sets can be treated as recording the same surface elevation on the concrete outfall and, given they consist of

374   three different surveys in time, are assumed to represent the 'true' surface elevation. This also suggests that

375   despite visible traces of sinking in of the ATV-GNSS system on the beach (Fig. 2), this has no measurable

376   impact on overall elevations which also include areas with a firmer surface.

377   Comparison of ALS with both the GNSS surveys on the concrete shows small differences and the lowest

378   RMSE values of the three contactless methods. This is evidence for the robustness of the survey grade ALS

379   equipment and ideal conditions of the test surface in relation to the near vertical laser beam on the aircraft

380   platform.The ALS – GNSS comparison on the beach surface (Table 1) also shows the best agreement in

381   elevation and the lowest RMSE values.

382   To provide a more consistent comparison for all tests, Table 3 summarises all results in relation to the ALS

383   survey as it is common to all comparisons including the point cloud only comparisons and provides the best

384   representation of the true surface owing to the consistency and spatial homogeneity of the dataset.

385

386

387   **Table 3**

388   Elevation differences from Table 2 and Figs 5, 6 and 9 converted into elevation differences relative to ALS. Negative

389   values mean that the method in the column heading was lower, positive that it was higher than ALS; for example, on

390   the concrete surface the MLS data was on average 0.056 m higher than the ALS data using the W-GNSS comparison and

391 0.068 m higher using the ATV-GNSS comparison. For the point cloud comparison results of UAS and MLS, the RMSE

392 value is also shown in parentheses. * indicates differences calculated indirectly for ATV and W-GNSS based on the ATV-

393 and W-GNSS comparison on the concrete outfall of -0.026 m.

Elevation differences in m	UAS		MLS		W-GNSS	ATV-GNSS
ALS concrete (W-GNSS)	0.007		0.056		-0.016	-0.021*
ALS concrete (ATV-GNSS)	0.008		0.068		-0.021*	-0.026
ALS beach (W-GNSS)	0.0531		0.011		0.0001	-0.0049*
ALS beach (ATV-GNSS)	0.064		0.006		0*	-0.005
ALS beach cloud (figs 5, 6 and 9)	0.063	(0.101)	-0.025	(0.069)	-	-
Gravel	0.038	(0.087)	-0.005	(0.063)		
Beach Sand	0.043	(0.08)	-0.042	(0.07)		
Cobble	0.118	(0.0.123)	0.056	(0.088)		
Dry sand	0.052	(0.072)	-0.05	(0.083)		
Wet sand	0.006	(0.073)	-0.05	(0.076)		
Soft mud	0.019	(0.072)	-0.089	(0.122)		
DEM 0.2 m grid	0.07		0.02			
DEM 0.5 m grid	0.08		0.01			
DEM 1 m grid	0.08		0.05			

394

395 On the concrete surface, the UAS data had a very low systematic error, but exhibited a wide scatter resulting

396 in a higher RMSE. It is suggested that the low optical contrast of the surface (either clean concrete or with a

397 cover of *enteromorpha sp.* algae, Fig. 11) is a possible reason for this, causing individual point errors in the

398 image matching process that, however, eventually cancel each other out. The MLS data exhibits a systematic

399 offset and RMSE outside of what could be expected from GNSS uncertainty. Inspecting the point cloud for

400 the MLS data on the outfall (Fig. 11), it is apparent that the outfall test surface was only covered by one pass

401 of the MLS ATV as it travelled in a northeast-southwest direction on the beach above the concrete surface,

402 so that the point density changed significantly with distance over the concrete surface and the incidence

403 angle became very shallow as the ATV moved down the beach. The average elevation of the outfall is 1.39

404 mOD which is reflected in the landward portion of the MLS data, but elevation increases with distance from

405   the instrument seawards. This highlights that in contrast to ALS, where due to the flying height and scan

406   angle the maximum angle between a horizontal surface and the laser beam is 25° with only a small

407   difference in distance between instrument and surface along the swath, the incidence angle and distance on

408   the MLS changes dramatically with every rotation of the scan head. This is generally compensated for in the

409   data processing by combining the data from several passes across the same area from different angles but in

410   the case of a single pass over a smooth and partly moist surface at a shallow angle, the results are not very

411   reliable.
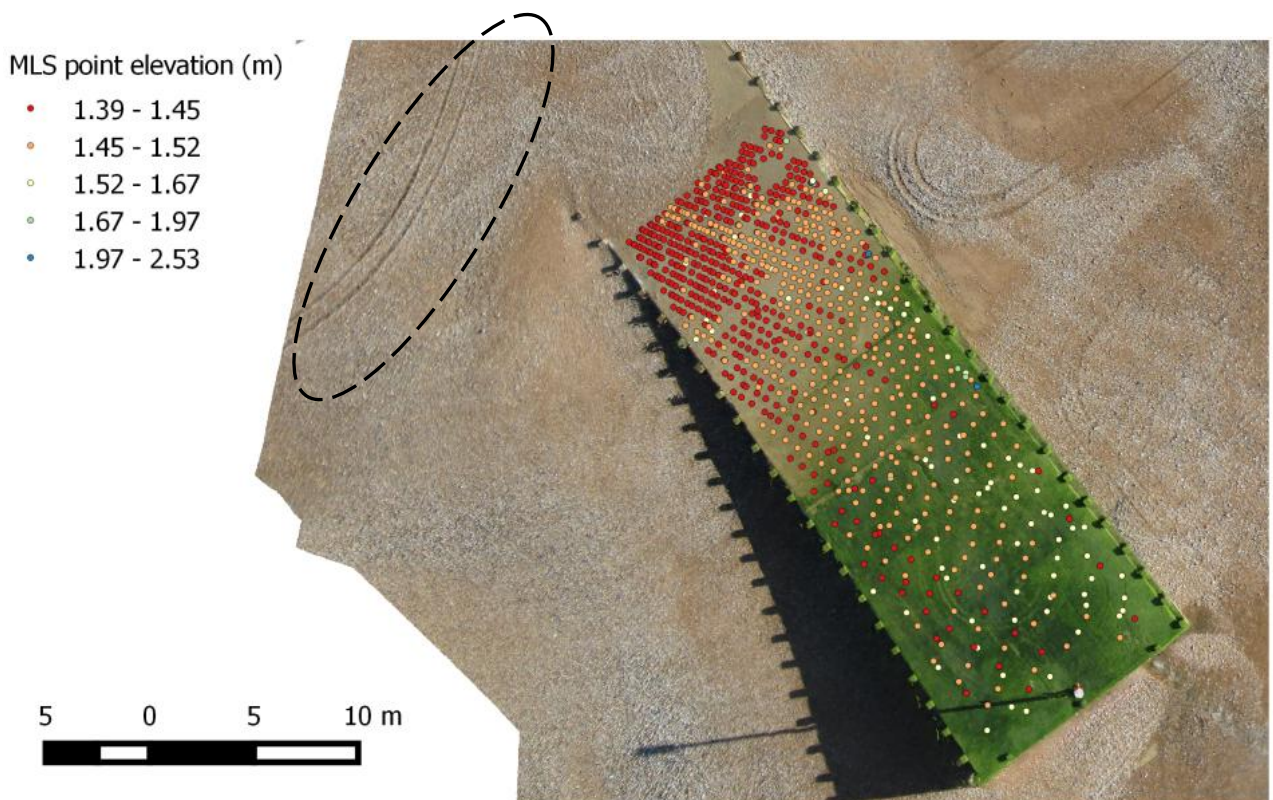
412

413   **Fig. 11.** Footprint of the mobile laser scanner (MLS) data on the concrete test surface of the sluice outfall, with dense

414   regular pattern at landward end and increasingly lower resolution towards the seaward end. Ellipse in the top left

415   highlights the track of the ATV carrying the laser scanner.

416   The analysis comparing point cloud data against RTK-GNSS data on the actual beach area introduces

417   additional error sources due to the interaction between the surface and the equipment, and the timing of

418   the surveys. The contact based methods (W-GNSS and ATV-GNSS) are shown to sink into the surface of the

419   study area depending on the type of surface and the weight of the equipment; surface micro topography

420 increases from a smooth sand surface to a sand surface with ripples to gravel to cobbles; wet sand provides a

421 different reflectivity to dry surfaces and the sequence in which the surveys were carried out meant that the

422 contactless methods picked up at least some of the traces left by the contact methods and the MLS (Fig. 2) .

423 Further to the surface roughness, the surface porosity changes and while the contact methods record the

424 highest points of the surface (albeit this is possibly overcompensated for by the sinking in), the MLS with its

425 laser footprint in the millimetre to centimetre range will return an elevation that is a composite but possibly

426 be slightly below a surface of the highest points.

427 The comparisons on the beach in Table 3 show again how close ALS and the two GNSS methods are with

428 negligible differences and RMSE values of 0.03 m and 0.036 m only about 0.01 m higher than on the concrete

429 surface (Table 2). The comparison also confirms indirectly (because there were no common points between

430 W-GNSS and ATV-GNSS within 0.1m on the beach) the high degree of agreement found between both

431 contact methods on the concrete surface. It also suggests that the visible sinking in of the ATV-GNSS does

432 not seem to impact the surface elevation. While the MLS data is significantly higher on the concrete outfall

433 surface it is very close to the ALS on the entire beach, being only 0.011 m (based on the W-GNSS

434 comparison) and 0.006 m (based on the ATV-GNSS comparison) higher. However, while the multiple paths

435 covering each part of the beach serve to bring the average closer to the true surface, the inherent

436 uncertainty of each individual point measurement results in a very high RMSE of 0.145 m and 0.113 m for

437 the W-GNSS and ATV-GNSS comparisons, respectively.

438 In contrast to the MLS data, the UAS data shows very little systematic difference on the concrete surface but

439 a significant difference on the overall beach of 0.0531 m and 0.064 m (RMSE values of 0.113 m 0.108 m) in

440 relation to the W-GNSS and ATV-GNSS comparisons, respectively.

441 Other than the comparison using the two GNSS surveys, where common points only exist for the comparison

442 pair with the 0.1 m radius, the point cloud comparison is based on common points for all three point clouds

443 within the 0.1 m radius resulting in 1960 point groups (Fig. 9). This point cloud comparison results in a very

444 similar difference compared to that based on the GNSS surveys for ALS and UAS (systematic offset of 0.063

445 m) but for the MLS comparison a previously subtle positive offset changes to an overall negative offset of -

446 0.025 m that falls outside of what is attributable to GNSS uncertainty and as this was not picked up in any of

447 the other comparisons appears to be an offset due to the MLS method. Breaking down the overall beach into

448 different surface components provides additional insight. The areas identified as belonging to a certain

449 surface type taken together are smaller than the entire beach area (Fig. 8 and Table 3) with the remaining

450 area not identified nevertheless belonging predominantly to the 'gravel', 'beach sand', 'dry sand' and 'wet

451 sand' types. As a consequence, these types contribute a large part of the offset. For the UAS data, these

452 types have a lower offset than the total beach which is disproportionally influenced by the relatively small

453 areas of 'Cobble' which have a 0.118 m offset to the ALS data. Given the different size of ALS and UAS point

454 footprint, ALS will inevitably provide a more averaged elevation while feature matching of the UAS method

455 will pick up the individual cobbles, thus giving a higher elevation. This interpretation also applies to the MLS

456 data where the general negative difference changes to a large positive difference, suggesting that the MLS is

457 also picking out the cobbles rather than the lower areas between them. Overall, the comparison for different

458 surface types appears to influence the elevation measurements although the number of sample points is

459 quite low for the smaller surface types. For the MLS survey it would appear as if surfaces with higher

460 roughness and thus good returns even on shallow incident angles of the laser beam, like gravel, produce

461 elevations similar to ALS and GNSS, whereas smoother surfaces result in lower elevations or no returns (Fig.

462 4a). The MLS records the same differences for wet and dry sand which is most likely due to the fact that the

463 MLS survey was carried out about 1 hour before the UAS flight used to identify the different sand type areas,

464 at which point previously wet sand had dried off in the early morning sun. This means that the MLS survey

465 encountered the sand on the low tide terrace when it was still wet while the UAS survey was presented with

466 distinct surface types, highlighting the importance of timing in relation to survey type and results.

467 The spatial pattern of residuals in the UAS – ALS comparison in Fig. 7, also seen in the UAS-MLS comparison,

468 show on closer inspection of the UAS surface model that two images for that part of the beach had sub-

469 optimal lighting which resulted in lower contrast. This apparently caused a localised problem for the

470 elevation model of the SfM modelling process. Such problems have also been described by Flener et al.

471 (2013). This issue illustrates a more general weakness of photogrammetry-based UAV methods. Surfaces

472 with a heterogeneous and distinct texture are particularly well suited for a successful and efficient image

473 matching process (Baltsavias, 1999). Reflective and/or homogeneous surfaces, however, are a more

474 problematic challenge for the feature matching stage, leading to a higher numbers of erroneous outliers

475 (Agisoft Photoscan, 2015; Fonstad et al., 2013). Surfaces such as concrete, sand, mud or gravel are examples

476 of such optical homogeneity and are therefore challenging for SFM approaches. This might explain the

477 relatively modest performance of the UAV point cloud when validated to GNSS measurements. In favourable

478 conditions, the RMSE of SFM-based point clouds can expected to be in the range of 1-2 multiples of the GSD.

479 In the on-hand project, the RMSE was 3 GSD concrete test surface and 6-7 GSD on the study area. This

480 corresponds to the performance of other coastal applications such as a UAV survey of beach dune systems

481 where the GSD multiple of the RMSE was even higher (Mancini et al., 2013).

482 Some authors recommend therefore to avoid potentially challenging surfaces in SFM-based monitoring

483 altogether (Micheletti et al., 2015b). However, this is often not practical in the operational monitoring

484 context. Instead, users need to aware that less confidence can be placed in the results of optically

485 problematic surfaces. An interesting method to address this problem is the addition of a near-infrared (NIR)

486 channel to the UAV sensor, as was done in the context of snow monitoring (Bühler et al., 2017). This led to a

487 significantly better performance during the image matching process. Such an approach might also be

488 promising in the coastal context.

489 When it comes to gridding the data into DEMs, the UAS-ALS difference from the point comparison (0.063 m)

490 translates into slightly higher positive values of 0.007 m to 0.008 m, irrespective of the grid size. In contrast,

491 the small negative difference between MLS and ALS transforms into a positive difference of between 0.01 m

492 and 0.05 m. The most likely reason for this is that significant shore-parallel areas of the low tide terrace have

493 no MLS data (Figure 4a) and so the interpolation starts from the shingle beach toe. Depending on the grid

494 size and grid position, this last elevation for the beach around the beach toe is likely to be higher than the

495 elevation of the low tide terrace just seawards of the beach toe leading to a large area of interpolated higher

496 surface. The irregular intersection between the rectilinear grid and the slightly oblique running beach toe is

497 likely to create the non-linear increase in average elevation, but the general increase of the 1m grid over the

498 other two is consistent, as the average elevation from points in a larger grid size on a slope will result in a

499 higher elevation for that grid cell.

5. Conclusion

501 This work presents, to the best knowledge of the authors, the first comparison of UAS, MLS and ALS data

502 collected at the same time on the same beach together with two GNSS methods to provide additional

503 ground reference data. The results indicate that ALS is overall the most robust method owing to its maturity

504 reflected in high instrument specification and long established and perfected flight planning and post

505 processing as well as optimum orientation between instrument and object with relatively low incident

506 angles. Bringing a laser scanner close to the ground as in the MLS increases the incidence angle with the

507 surface dramatically, resulting in poorer reflection and, as a consequence, a much wider scatter of the data.

508 Adding to this, the additional error terms associated with the GNSS and IMU on a fast moving vehicle over

509 uneven ground produce the highest RMSE. Apart from on the concrete control surface, UAS elevations were

510 consistently higher than ALS and, as a consequence the true surface elevation, by about 0.05 m with RMSE

511 values about halfway between ALS and MLS. Individual spatial patterns of larger or smaller differences than

512 the average appear to be related to sediment characteristics with some more suited, for example, to the

513 pattern recognition of the UAS method or the better reflectivity of oblique incident laser pulses, while others

514 create more difficulty due to surface homogeneity or poor reflectivity.

515 Generally, the more instruments or processes and the less time available to produce the co-ordinate, the

516 larger the RMSE. This is illustrated by the low RMSE for the GNSS instruments sampling at 1Hz which

517 increases for the UAS due to uncertainties of the camera and image quality influenced by lighting conditions,

518 inferred camera position, image matching and co-ordinate calculation in addition to the overall geo-

519 referencing using GNSS as ground control or on board. The MLS has the highest RMSE despite only using

520 three instruments (GNSS, laser, IMU). The speed of movement of the instrument comparatively close to the

521 surface it is measuring together with the shallow angle of incidence lead to large point density but also high

522 uncertainty as regards the location of each individual point.

523 The ALS system has the same number of components as the MLS, but the much smaller RMSE is a result of

524 the more stable platform, more favourable position of the more sophisticated instrument in relation to the

525 measured object. However, this also comes with significantly higher investment and operating costs.

526 The comparison shows that all methods produce elevations that can be used for operational monitoring

527 beach topography changes. This means that UAS represent a viable, low cost and flexible alternative to laser

528 scanning approaches. In addition to this, UAS have the added advantage that they collect multi-spectral

529 image information about the surface under investigation. This secondary data set that can be used to, e.g.

530 analyse the distribution of sand and gravel sections of the upper beach at Pevensey Bay.

531 However, when monitoring the same beach repeatedly, care needs to be taken to ensure that the data

532 collected is sufficient for later analysis. In the case of UAS, the number of overlapping images needs to be

533 extended beyond the actual area of the survey to avoid any edge effects from insufficient overlap creeping

534 into the survey area. In addition, data quality (in this case the image quality analogue to the PDOP on GNSS

535 equipment) must be checked during capture so that it can be reflown immediately if the quality is not

536 satisfactory. In the case of the MLS, it requires ensuring that the same area is covered by several passes with

537 different incident angles and recognising that some surfaces like wet sand may not produce a return even in

538 close proximity to the scanner.

539 Given that in terms of accuracy all methods produce comparable results, the choice of UAS as operational

540 monitoring method is likely to be guided by practical considerations:

541 • cost of the survey (capital cost of the system and operating costs per survey area),

542 • conditions under which the system can operate (e.g. wind, light levels, visibility despite clouds, fog or

543 sea spray in the air),

544 • size and shape of the survey area and time window available for the survey,

545 • ease of calling off the system for a survey,

546 • processing time between the survey and the data becoming available,

547 • restrictions in the use of the system (e.g. regulations relating to airborne systems or ground access

548   to areas with environmental protection),

549 • additional benefits such as orthophoto creation, surface type analysis or coincident use of other

550   instruments (for example infrared cameras),

551 • required accuracy for smaller sub areas or

552 • point density.

553 Some of these factors will depend on the UAS platform, as rotary and fixed wing set-ups have different

554 sensitivities to wind conditions shape of the survey area, or flying speed. Of further importance is the

555 country it is used in, and its regulations on UAS use. The weighting of each of these factors will depend on

556 the monitoring project and its objectives. UAS will in many cases be the method of choice, but as with every

557 new method, especially if it replaces another method used to create data for the same location before, tests

558 about comparability of the data collected with both methodologies are essential.

559 Some monitoring projects, like the English Network of Coastal Monitoring Programmes covers the same

560 coastline with different methods at different times such as ATV-GNSS, MLS, ALS and static terrestrial laser

561 scanning. As the research reported here demonstrates, there can be systematic differences between

562 respective monitoring approaches. This means when a mix of survey methods is used, a better

563 understanding of such effects is necessary and future research should investigate more systematically such

564 sensitivities on e.g. the calculation of beach volumes differences.

565 **Acknowledgements**

570

References:

572   Agisoft Photoscan, 2015. Agisoft Photoscan User Manual - Optimisation. Version 1.2.3.

573   Anderson, J.M., Anderson, J.M., Mikhail, E.M., 1998. Surveying, theory and practice. McGraw-Hill
574   Science/Engineering/Math.

575   Baltsavias, E., 1999. A comparision between photogrammetry and laser scanning. ISPRS J. Photogramm.
576   Remote Sens. 54, 83–94.

577   Brunier, G., Fleury, J., Anthony, E.J., Gardel, A., Dussouillez, P., 2016. Close-range airborne Structure-from-
578   Motion Photogrammetry for high-resolution beach morphometric surveys: Examples from an embayed
579   rotating beach. Geomorphology 261, 76–88. doi:10.1016/j.geomorph.2016.02.025

580   Bühler, Y., Adams, M.S., Stoffel, A., Boesch, R., 2017. Photogrammetric reconstruction of homogenous snow
581   surfaces in alpine terrain applying near-infrared UAS imagery. Int. J. Remote Sens. 38, 3135–3158.
582   doi:10.1080/01431161.2016.1275060

583   Delgado, I., Lloyd, G., 2004. A simple low cost method for one-person beach profiling. J. Coast. Res. 20, 1246–
584   1252.

585   Dornbusch, U., 2010. Ground survey methods for mixed sand and gravel beaches in intertidal environments:
586   a comparison. J. Coast. Res. 26, 451–464. doi:DOI: 10.2112/08-1134.1

587   Dornbusch, U., Robinson, D., Moses, C., Williams, R.B.., 2008. Variation in beach behaviour in relation to
588   groyne spacing and groyne type for mixed sand and gravel beaches, Saltdean, UK. Zeitschrift für
589   Geomorphol. N.F. 52, 125–143.

590   Eitel, J.U.H., Höfle, B., Vierling, L.A., Abellán, A., Asner, G.P., Deems, J.S., Glennie, C.L., Joerg, P.C., LeWinter,
591   A.L., Magney, T.S., Mandlburger, G., Morton, D.C., Müller, J., Vierling, K.T., 2016. Beyond 3-D: The new
592   spectrum of lidar applications for earth and ecological sciences. Remote Sens. Environ. 186, 372–392.
593   doi:10.1016/j.rse.2016.08.018

594   Flener, C., Vaaja, M., Jaakkola, A., Krooks, A., Kaartinen, H., Kukko, A., Kasvi, E., Hyyppä, H., Hyyppä, J., Alho,
595   P., 2013. Seamless mapping of river channels at high resolution using mobile liDAR and UAV-
596   photography. Remote Sens. 5, 6382–6407. doi:10.3390/rs5126382

597   Fonstad, M.A., Dietrich, J.T., Courville, B.C., Jensen, J.L., Carbonneau, P.E., 2013. Topographic structure from
598   motion: A new development in photogrammetric measurement. Earth Surf. Process. Landforms 38,
599   421–430. doi:10.1002/esp.3366

600   Girardeau-Montaut, D., 2015. CloudCompare version 2.6.1. user manual 181.

601   Gonçalves, J.A., Henriques, R., 2015. UAV photogrammetry for topographic monitoring of coastal areas.
602   ISPRS J. Photogramm. Remote Sens. 104, 101–111. doi:10.1016/j.isprsjprs.2015.02.009

603   Goncalves, R.M., Awange, J., Krueger, C.P., 2012. GNSS-based monitoring and mapping of shoreline position
604   in support of planning and management of Matinhos/PR (Brazil). J. Glob. Position. Syst. 11, 156–168.

605   Harwin, S., Lucieer, A., 2012. Assessing the accuracy of georeferenced point clouds produced via multi-view
606   stereopsis from unmanned aerial vehicle (UAV) imagery. Remote Sens. 4, 1573–1599.

607   Klemas, V. V, 2015. Coastal and environmental remote sensing from unmanned aerial vehicles: An overview.
608   J. Coast. Res. 31, 1260–1267.

609   Lim, M., Dunning, S.A., Burke, M., King, H., King, N., 2015. Quantification and implications of change in
610   organic carbon bearing coastal dune cliffs: A multiscale analysis from the Northumberland coast, UK.
611   Remote Sens. Environ. 163, 1–12. doi:10.1016/j.rse.2015.01.034

612   Mancini, F., Dubbini, M., Gattelli, M., Stecchi, F., Fabbri, S., Gabbianelli, G., 2013. Using unmanned aerial

613   vehicles (UAV) for high-resolution reconstruction of topography: The structure from motion approach
614   on coastal environments. Remote Sens. 5, 6880–6898. doi:10.3390/rs5126880
615 Micheletti, N., Chandler, J.H., Lane, S.N., 2015a. Investigating the geomorphological potential of freely
616   available and accessible structure-from-motion photogrammetry using a smartphone. Earth Surf.
617   Process. Landforms 40, 473–486. doi:10.1002/esp.3648
618 Micheletti, N., Chandler, J.H., Lane, S.N., 2015b. Structure from Motion (SfM) Photogrammetry.
619   Geomorphol. Tech. 2, 1–12. doi:10.5194/isprsarchives-XL-5-W4-37-2015
620 Nex, F., Remondino, F., 2014. UAV for 3D mapping applications: a review. Appl. Geomatics 6, 1–15.
621   doi:10.1007/s12518-013-0120-x
622 Oborne, M., n.d. Mission Planner Overview | Mission Planner [WWW Document]. URL
623   http://planner.ardupilot.com/wiki/mission-planner-overview/ (accessed 3.8.16).
624 Papakonstantinou, A., Topouzelis, K., Pavlogeorgatos, G., 2016. Coastline Zones Identification and 3D Coastal
625   Mapping Using UAV Spatial Data. ISPRS Int. J. Geo-Information 5, 75. doi:10.3390/ijgi5060075
626 Pereira, E., Bencatel, R., Correia, J., Félix, L., Gonçalves, G., Morgado, J., Sousa, J., 2009. Unmanned air
627   vehicles for coastal and environmental research. J. Coast. Res. 1557–1561.
628 Renishaw, 2016. Data sheet: Dynascan M250.
629 Turner, I.L., Harley, M.D., Drummond, C.D., 2016. UAVs for coastal surveying. Coast. Eng. 114, 19–24.
630   doi:10.1016/j.coastaleng.2016.03.011
631 Watt, T., Robinson, D., Moses, C., Dornbusch, U., 2008. Patterns of surface sediment grain size distribution
632   under the influence of varying wave conditions on a mixed sediment beach at Pevensey Bay, southeast
633   England. Zeitschrift für Geomorphol. - Suppl. 52, 63–77.
634 Westoby, M.J., Brasington, J., Glasser, N.F., Hambrey, M.J., Reynolds, J.M., 2012. "Structure-from-Motion"
635   photogrammetry: A low-cost, effective tool for geoscience applications. Geomorphology 179, 300–314.
636   doi:10.1016/j.geomorph.2012.08.021
637
638

639

640